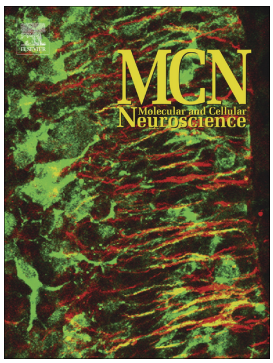

A proteomic investigation into mechanisms underpinning corticosteroid effects on neural stem cells

Rawaa S. Al-Mayyahi, Luke D. Sterio, Joanne B. Connolly, Christopher F. Adams, Wa'il A. Al-Tumah, Jon Sen, Richard D. Emes, Sarah R. Hart, Divya M. Chari

PII: S1044-7431(17)30043-X
DOI: doi:10.1016/j.mcn.2017.11.006
Reference: YMCNE 3247

To appear in: *Molecular and Cellular Neuroscience*

Received date: 10 February 2017
Revised date: 3 November 2017
Accepted date: 6 November 2017

Please cite this article as: Rawaa S. Al-Mayyahi, Luke D. Sterio, Joanne B. Connolly, Christopher F. Adams, Wa'il A. Al-Tumah, Jon Sen, Richard D. Emes, Sarah R. Hart, Divya M. Chari , A proteomic investigation into mechanisms underpinning corticosteroid effects on neural stem cells. The address for the corresponding author was captured as affiliation for all authors. Please check if appropriate. Ymcne(2017), doi:10.1016/j.mcn.2017.11.006

A proteomic investigation into mechanisms underpinning corticosteroid effects on neural stem cells

Rawaa S. Al-Mayyahi[a], Luke D. Sterio[c], Joanne B Connolly[d], Christopher F. Adams[a], Wa'il A. Al –Tumah[a], Jon Sen[e], Richard D. Emes[b¥], Sarah R. Hart[a¥], Divya M. Chari[a*¥]

[a]Institute for Science and Technology in Medicine, Keele University, Keele, Staffordshire, ST5 5BG, UK

[b]Advanced Data Analysis Centre, University of Nottingham, Sutton Bonnington, Leicestershire, LE12 5RD, UK

[c]School of Medicine, David Weatherall Building, Keele University, Staffordshire, ST5 5BG, UK.

[d]Waters Corporation, Altrincham Rd, Wilmslow SK9 4AX

[e]Walton Centre for Neurology and Neurosurgery, Liverpool, L9 7BB

*Corresponding author: Professor Divya M. Chari

¥ Authors contributed equally

E-mail: d.chari@keele.co.uk

Tel: 00-44-1782-733314

Fax: 00-44-1782-734634

Abstract

Corticosteroids (CSs) are widely used clinically, for example in paediatric respiratory distress syndrome, and immunosuppression to prevent rejection of stem cell transplant populations in neural cell therapy. However, such treatment can be associated with adverse effects such as impaired neurogenesis and myelination, and increased risk of cerebral palsy. There is increasing evidence that CSs can adversely influence key biological properties of neural stem cells (NSCs) but the molecular mechanisms underpinning such effects are largely unknown. This is an important issue to address given the key roles NSCs play during brain development and as transplant cells for regenerative neurology. Here, we describe the use of label-free quantitative proteomics in conjunction with histological analyses to study CS effects on NSCs at the cellular and molecular levels, following treatment with methylprednisolone (MPRED). Immunocytochemical staining showed that both parent NSCs and newly generated daughter cells expressed the glucocorticoid receptor, with nuclear localisation of the receptor induced by MPRED treatment. MPRED markedly decreased NSC proliferation and neuronal differentiation while accelerating the maturation of oligodendrocytes, without concomitant effects on cell viability and apoptosis. Parallel proteomic analysis revealed that MPRED induced downregulation of growth associated protein 43 and matrix metallopeptidase 16 with upregulation of the cytochrome P450 family 51 subfamily A member 1. Our findings support the hypothesis that some neurological deficits associated with CS use may be mediated via effects on NSCs, and highlight putative target mechanisms underpinning such effects.

Keywords: Corticosteroid, neural stem cell, neural cell, proteomics

Abbreviations

CS, corticosteroid; CNS, central nervous system; NSCs, neural stem cells; SCI, spinal cord injury; MPRED, methylprednisolone; NPCs, endogenous neural progenitor cells; FGF2, Human recombinant basic fibroblast growth factor; EGF, epidermal growth factor; TUJ 1, neuron specific class III β-tubulin; GFAP, glial fibrillary acidic protein; MBP, myelin basic protein; DAPI, 4′, 6-diamidino-2-phenylindole; Ambic, Ammonium Bicarbonate; SVZ, subventricular zone; DMEM, Dulbecco's Modified Eagle Medium; DMSO, dimethyl sulfoxide; PBS, phosphate buffered saline; PFA, paraformaldehyde; RT, room temperature; Edu, 5-ethynyl-2'-deoxyuridine; FBS, fetal bovine serum; IPA, Ingenuity Pathway Analysis; GRs, glucocorticoid receptors; MMP-16, matrix metallopeptidase -16; GAP-43, growth associated protein 43; CYP51A1, cytochrome P450 family 51 subfamily A member 1; ECM, extracellular matrix; OPCs, oligodendrocyte precursor cells.

1. Introduction

Corticosteroids (CSs) are a group of small lipid-soluble molecules which readily pass through the blood-brain-barrier and exert physiological effects on the central nervous system (CNS) (Riedemann et al., 2010). Their responses are mediated by binding to a member of the nuclear receptor superfamily of transcription factors called glucocorticoid receptors (GRs) to form a cytoplasmic complex (Ayroldi et al., 2012; Rhen and Cidlowski, 2005). This complex migrates to the nucleus and binds directly to DNA sequences termed glucocorticoid response elements (GRE) in the promoter region, or other DNA bound transcription factors. This results in increased target gene expression such as for anti-inflammatory-proteins (transactivation), or reduced production of pro-inflammatory proteins (transrepression) (Rhen and Cidlowski, 2005).

The therapeutic effects of CSs as anti–inflammatory and immunosuppressive drugs have employed since the 1950s (Chari, 2014; Shinwell and Eventov-Friedman, 2009) to treat diverse pathologies such as asthma, allergies and rheumatoid arthritis (Rhen and Cidlowski, 2005). In neural cell transplantation therapy, the use of anti-inflammatory and immunosuppressive drugs such as CSs is essential to improve transplant survival and limit rejection by host tissue (Mazzini et al., 2015; Skardelly et al., 2013). Research has however highlighted several adverse effects of CSs, including elevated risks of neurodevelopmental impairment, cerebral palsy and cognitive impairment (Chari, 2014; Heine and Rowitch, 2009; Shinwell and Eventov-Friedman, 2009). These risks are increased by prolonged and high exposure treatment, which can lead to structural changes in neurons and reduced neurogenesis, especially in the hippocampus, where inhibition of cell proliferation and increased cell death are observed in the dentate gyrus (Heberden et al., 2013).

Several *in vivo* and *in vitro* experimental studies suggest that at least some such adverse effects are mediated via effects on neural stem cells (NSCs) - self-renewing, multipotent cells that generate the major CNS cell types (astrocytes, neurons and oligodendrocytes). Extensive research shows that NSCs plays key roles in brain development and endogenous/transplant mediated repair (Skardelly et al., 2013). However, CS treatment can reduce NSC proliferation (a key underpinning of their regenerative effects) with aberrations in fetal and adult neurogenesis (Bose et al.,2010; Kim et al., 2004; Sundberg et al., 2006). Similarly, Bose *et al.* suggested that NSC exposure to CSs could reduce their proliferation without effects on survival/differentiation, whereas Moore and colleagues observed CS-mediated decreases in both the proliferation and differentiation of human NSCs (Bose et al., 2010; Moors et al., 2012). Some studies have demonstrated that methylprednisolone (MPRED) can reduce endogenous neural progenitor cell proliferation in the spinal cord following traumatic SCI (Obermair et al., 2008).

Given widespread clinical CS use, and the key roles of NSCs in developmental and regenerative processes, these findings highlight a significant need to investigate the mechanisms mediating CS effects on NSCs. Despite this, it should be noted that the overwhelming majority of studies investigating CS effects on NSCs rely exclusively on histological analyses. Whilst useful, such assays cannot provide detailed insight into the potential molecular mechanisms underpinning the observed neurological effects on NSCs. Here, we have adopted a dual methodological approach, employing parallel histological and proteomic analyses on CS-treated NSCs to address this issue. This allows us to generate independently validated and corroborative analyses of CS effects at both the morphological and molecular levels**.**

2. Materials and methods

2.1. Reagents

Cell culture reagents were from Life Technologies (Paisley, Scotland, UK) and Sigma-Aldrich (Poole, Dorset, UK). Nunc culture dishes (non-treated surface) and tissue culture-grade plastics were from Fisher Scientific (Loughborough, UK). Human recombinant basic fibroblast growth factor (FGF2) and epidermal growth factor (EGF) were from Sigma-Aldrich and R&D Systems Europe Ltd (Abingdon, UK), respectively. The following primary antibodies were used: Nestin (NSC specific marker; BD Biosciences, Oxford, UK), glial fibrillary acidic protein (GFAP – astrocytes; DakoCytomation, Ely, UK), neuron specific class III β-tubulin (TUJ 1- neurons; Covance, Princeton, NJ) and myelin basic protein (MBP – oligodendrocytes; Serotec, Kidlington, UK). Two glucocorticoid receptor antibodies H-300 and BuGR2 were from Santa Cruz Biotech (USA) and Abcam (UK), respectively. A neuronal marker rabbit anti- growth associated protein (GAP 43) was from (Abcam, UK). Secondary antibodies (Cy3- FITC-conjugated) were from Jackson Immunoresearch Laboratories Ltd (Westgrove, PA, USA). DAPI (4', 6-diamidino-2-phenylindole) mounting medium was from Vector Laboratories (Peterborough, UK). 6-α-methylprednisolone (≥98% purity) was from Sigma. Click-iT1 Edu Alexa Fluor kit was from Life Technologies, the LIVE/DEAD Viability/Cytotoxicity Assay Kit was from Invitrogen. Kits for cell cycle and Annexin V and Dead cell were from Millipore (Watford, UK). Trifluoroacetic acid was from Fisher Scientific. Acetonitrile was from VWR Chemicals (Lutterworth, UK), Iodoacetamide was from Acros Organics (Geel, Belgium) and Rapigest was from Waters Corporation (Altrincham, UK). Ammonium Bicarbonate (Ambic), protease inhibitor

cocktail, dithiothreitol, Proteomics-Grade dimethylated trypsin and Bradford Reagent were from Sigma.

2.2. Isolation and culture of NSCs

The care and use of all animals used in the production of cell cultures were in accordance with the Animals Scientific Procedures Act of 1986 (UK) with approval by the local ethics committee.

NSCs were derived from the subventricular zone (SVZ) of CD1 mouse pups, post-natal day 1-3 (the day of birth was designated as postnatal day 0) (Adams et al., 2013). Briefly, under sterile conditions, sections containing SVZ were obtained. Tissue was mechanically dissociated into a single cell suspension in the presence of DNase I, cells were counted and plated at 1 x 10^5 cells/ml in neurosphere medium: 3:1 mix Dulbecco's Modified Eagle Medium (DMEM):F12 supplemented with 2% B27 supplement, 20 ng/ml FGF2 and EGF, 4 ng/ml heparin, 50 U/ml penicillin, 50µg/ml streptomycin. Cultures were fed every 2-3 days and passaged every 5-7 days using a mix of accutase and DNase I. For adherent cultures, neurospheres were dissociated and plated on poly-L-ornithine and laminin coated coverslips and maintained in monolayer medium which was prepared with a 1:1 mix DMEM: F12, 1% N2 supplement 20 ng/ml FGF-2 and EGF, 5 µg/ml heparin, 50 U/ml penicillin and 50 µg/ml streptomycin.

2.3. Preparation of MPRED solution

The synthetic CS, MPRED is one of the main drugs used in the treatment of neurological trauma (acute SCI and traumatic brain injury) because of its ability to reduce brain edema, improve neurological recovery and reduce the inflammatory reaction after SCI (Han et al., 2014). This drug was therefore selected for use in

these experimental studies. MPRED stock was prepared in dimethyl sulfoxide (DMSO) with the concentration verified spectrophotometrically (Genesys 10S UV−vis spectrophotometer, ThermoScientific, USA) then diluted in culture medium to the appropriate concentration. The highest dose of MPRED (10 µM) was used for further proteomic analysis.

2.4. MPRED treatment of NSCs

NSCs were cultured as adherent monolayers in 24-well plates at a density of 0.65 x 10^5 cells/ ml (600 µl/well). One day after plating, NSCs were treated with MPRED by replacing cell culture medium with medium containing three different concentrations (0.1 µM, 1 µM and 10 µM) of MPRED followed by incubation for 48 h. The culture medium of untreated NSCs was replaced with fresh medium (without MPRED) and vehicle controls contained DMSO. Cells were then washed once in phosphate-buffered saline (PBS), fixed with 4% paraformaldehyde (PFA), [15 mins, room temperature (RT)], before washing a further 3X in PBS, unless detailed otherwise.

2.5. NSC proliferation assay

The 5-ethynyl-2'-deoxyuridine (Edu) assay was used to measure the effects of MPRED on cellular proliferation rates. Detection of Edu incorporation into the DNA was performed with Click-iT1 Edu Alexa Fluor proliferation assay kit, following the manufacturer's instructions. Briefly, 10 μM EdU in a final volume of 0.3 mL monolayer medium was added over the coverslip followed by incubation at 37° C for 16 h. This incubation time was determined by the cell doubling time for NSCs of around 20 h (Bose et al., 2010; Sun et al., 2009). Cells were fixed at 48 h post-MPRED treatment in 4% PFA for 20 min at RT, followed by 2 washes with 3% bovine serum albumen (BSA). Cells were permeabilsed by incubation for 20 min in 0.3% Triton-X 100 in PBS (0.5 mL). Then cells were washed twice in 3% BSA and the reagent cocktail for EdU detection was distributed over the cells. Following incubation at RT for 30 min (protected from light), the cells were washed twice with 3% BSA and mounted for fluorescence microscopy. Fluorescence images were captured from four random fields of the coverslip. Counts of nuclei co-expressing the EdU marker and nuclear counterstain (DAPI) were classified as proliferating cells (proliferation expressed as a percentage of the total cells counted).

2.6. Cell cycle analysis

Cell cycle analysis was performed at 48 h post-MPRED treatment. NSCs (1×10^6) were harvested, fixed with 1 ml of 70% cold ethanol and incubated at -20 °C for at least 3 h prior to staining, as per the Muse Cell Cycle Kit instructions. Subsequently, 200 μl of ethanol-fixed cells were washed in PBS and stained for 30 mins at RT in the dark with 200 μl of Muse Cell Cycle Reagent. Cell suspensions were transferred into 1.5 ml microcentrifuge tubes and analyzed using a Muse Cell Analyzer (EMD

Millipore, Darmstadt, Germany), with an automated readout of proportions of cells in each phase of the cell cycle.

2.7. Viability assay

NSC viability was measured at 48 h post-MPRED treatment using LIVE/DEAD viability/cytotoxicity kit which contains calcein AM and ethidium homodimer-1 (Ethd-1). Cells were washed with PBS, incubated for 15 mins with 4 µM calcein AM (produces green fluorescence in live cells) and 6 µM Ethd-1(produces red fluorescence in dead cells), dissolved in PBS. Cells were then washed again with PBS and mounted for fluorescence microscopy.

2.8. Apoptosis assay

Muse Annexin V and Dead cell kit was used to quantify apoptotic cells. After 48 h treatment of NSCs with MPRED, they were stained with Annexin V, following the manufacturer's instructions. 100 µl of cells in suspension were added to 100 µl of the Muse Annexin V and Dead cell reagent and stained for 20 mins at RT in the dark. Stained cells were measured by the Muse Cell analyzer.

2.9. NSC differentiation assay

To examine the effect of MPRED treatment on NSC differentiation, NSCs treated as in Section 2.4 were switched to differentiation medium [neurosphere medium without growth factors but with addition of 1% fetal bovine serum (FBS)] containing the same concentrations of MPRED. Cells were cultured for a further 7 days to allow differentiation. At the end of the total incubation time (9 days) cells were fixed with 4% PFA.

2.10. Immunocytochemistry

Following fixation, non-specific staining was blocked (blocking solution: 5% normal donkey serum, 0.3% Triton-X-100 in PBS) for 30 mins at RT. Primary antibodies were diluted as follows in blocking solution: Nestin 1:200, H300 1:100, BuGR2 1:100, β-tubulin III/TUJ-1 1:1000, GFAP 1:500, MBP 1:200, GAP 43 1:500, added to the cells and incubated overnight at 4°C. Stained cells were washed three times in PBS, blocked for 30 mins at RT and incubated with the appropriate FITC- or Cy3-conjugated secondary antibody in blocking solution (1:200 dilution, RT; 2 h), cells were then washed three times with PBS at RT, and mounted with DAPI.

2.11. Microscopy and image analysis

Fluorescence images were taken using an Axio Scope A1 microscope equipped with an Axio Cam ICc1 digital camera and AxioVision software (release 4.7.1, Carl Zeiss MicroImaging GmbH, Goettingen, Germany). Photoshop CS3 (Adobe, USA) was used to merge counterpart images; three channels were merged to form 'triple merge' images. At least four microscopic fields were captured per condition for subsequent analysis. The proportions of total numbers of cells expressing a specific neural cell markers was expressed versus total cell number estimated using DAPI nuclear staining, using ImageJ software. ImageJ software was also used to measure the lengths of the axon of neurons and the area occupied by oligodendrocytes. To validate proteomic findings regarding GAP 43 expression, fluorescence micrographs of control and CS-treated NSCs and their differentiated cells were converted to grayscale (Photoshop) and calibrated as a batch (optical density step-tablet, Rodbard equation; ImageJ, National Institutes of Health, USA). The relative expression of GAP 43 protein was quantified using optical density measurements of

individual cells (minimum of 30 nestin$^+$ NSCs and TUJ 1$^+$ neurons and four images per condition per culture), with background readings subtracted.

2.12. Statistical analysis of histological data

All data from the effects of MPRED on the NSC parent cells and their differentiated cells were analyzed using Prism statistical analysis software (GraphPad) and are presented as mean ± standard error of the mean (SEM). $P < 0.05$ was chosen as the level of statistical significance. Data were analyzed by one-way ANOVA with Bonferroni's multiple comparison tests (MCT) as appropriate. Optical density measurements of GAP 43 expression were compared using an unpaired t test. The numbers of experiments (n) relate to the number of NSC cultures, each generated from a different litter.

2.13. Proteomic and bioinformatics analyses

Proteomic analysis was performed to examine protein expression in NSCs; NSCs were plated as monolayers in 6 well plates at 1.2 x 10^5 cells/ml in 1.5 ml. These were left for one day to adhere and then treated with 10 µM MPRED for 48 h. In order to obtain protein from the NSCs, the cells were enzymatically detached using TrypLE (RT, <5 mins). Cells were pelleted by centrifugation and washed three times in 50 mM Ammonium Bicarbonate (Ambic) with centrifugation in between each wash. Cell pellets were dissolved in 100 µl lysis buffer (0.1% Rapigest, 1% DNAse I in 50mM Ambic), and cells were lysed using probe sonication. Cell debris was pelleted at 15,000 g for 5 mins and the protein concentration of the supernatant fraction of each lysate determined by Bradford assay according to manufacturer's protocol.

2.13.1. Tryptic digestion of cell lysate proteins

100 µg of each lysate was subjected to in-solution tryptic digestion. Each lysate was incubated with 10 mM dithiothreitol with shaking (80°C, 15 mins) before reduction using iodoacetamide (20 mM, 30 mins, RT, kept dark). Trypsin (2 µg) was then added to each sample, with incubation at 37°C for 16 h. Remaining tryptic activity was terminated, and Rapigest precipitated, by addition of trifluoroacetic acid (1% v/v) and acetonitrile (2% v/v) with shaking (60°C, 2 h). Rapigest was pelleted and removed by centrifugation at 15,000 g for 5 mins, with the supernatant being used for mass spectrometry.

2.13.2 Mass spectrometry

We performed data-independent high-definition MS^E analysis (Rodriguez-Suarez et al., 2013), with ion mobility separation of precursor and mixed pseudo-product ion

data using a Synapt G2Si instrument with associated NanoAcquity UPLC (Waters Corporation, Wilmslow, Cheshire) (Ansari et al., 2015; Burniston et al., 2014). Data were analysed using Progenesis QI for proteomics (Non-Linear Dynamics, Newcastle upon Tyne), with a High-N (n=3) quantification being used to generate quantification data (Silva et al., 2005). An ANOVA p value of 0.05 was used as a cut-off for significance of differential protein identifications. Pathway analysis to identify differentially-regulated proteins was performed using Ingenuity Pathway Analysis (IPA; QIAGEN, Redwood City CA, www.qiagen.com/ingenuity). Statistical enrichment is calculated by a right-tailed Fisher's exact test.

3. Results

3.1. GR expression in NSCs and their daughter cells

The parent NSC cultures routinely established in our experiments were of high purity: 97.7 (± 1.6) % nestin$^+$ NSCs. After differentiation, daughter cells were produced in the following proportions, judged by immunostaining for cell-specific markers [84.7 (± 2.1) % GFAP$^+$ astrocytes, 9.2 (± 0.2) % TUJ 1$^+$ neurons and 5.5 (± 0.2) % MBP$^+$ oligodendrocytes]. In our hands these are the expected ratios using the differentiation protocol described. Immunostaining showed positive staining for GR in all the cell types in control cultures (Fig. 1A, C, E and G). 10 μM MPRED treatments induced nuclear translocation of GR, with greater intensity of nuclear staining observed following drug application (Fig. 1B, D, F and H).

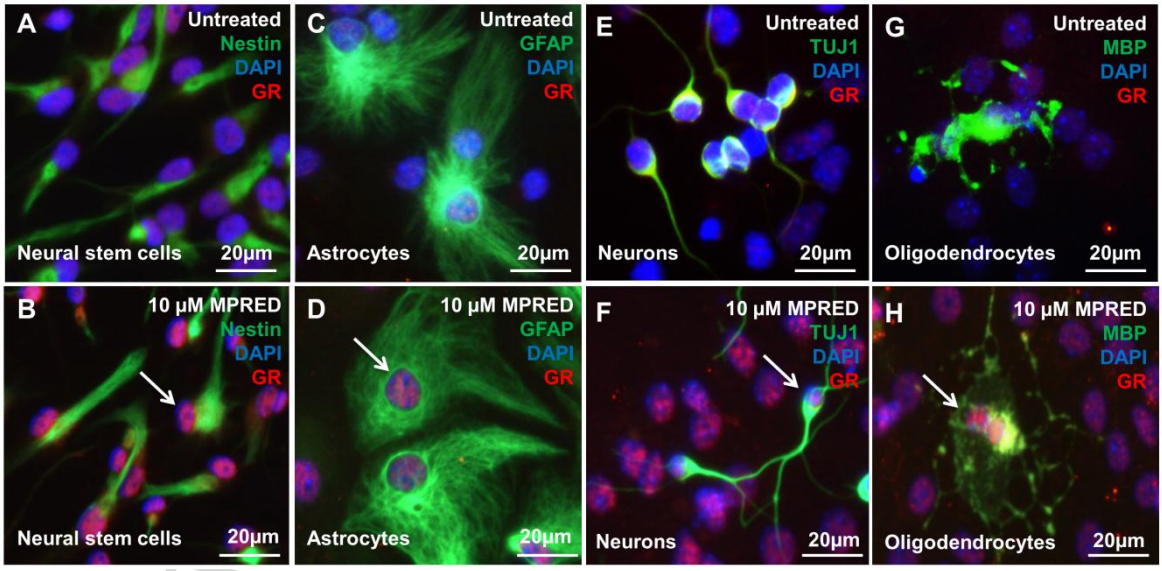

Fig. 1. NSCs and their daughter cells express GR. *Representative fluorescence micrographs showing GR expression in untreated cells (A, C, E and G): nestin$^+$ NSCs (A), GFAP$^+$ astrocytes (C), TUJ 1$^+$ neurons (E) and MBP$^+$ oligodendrocytes (G), compared with MPRED-treated cells (48 h MPRED, 10 μM, panels B, D, F and*

H): nestin$^+$ NSCs (B) GFAP$^+$ astrocytes (D), TUJ 1$^+$ neurons (F) and MBP$^+$ oligodendrocytes (H), n=3.

3.2. Effect of MPRED on the number, proportion and proliferation of NSCs

Immunostaining for nestin revealed that 10 μM MPRED significantly reduced the total counts of NSCs compared with control and vehicle (Fig. 2A, B and C). No differences in proportions of nestin positive cells were observed between control versus treatment conditions (Fig. 2D). 10 μM MPRED also significantly decreased the percentage of Edu$^+$ (proliferative) cells (Fig. 2E, F and G). Cell cycle analysis showed that in parallel with reduced proliferation, 10 μM MPRED led to a significant increase of cells in the G0/G1 phase with a parallel decrease of cells in S and G2/M phases, compared with controls (Fig. 2H).

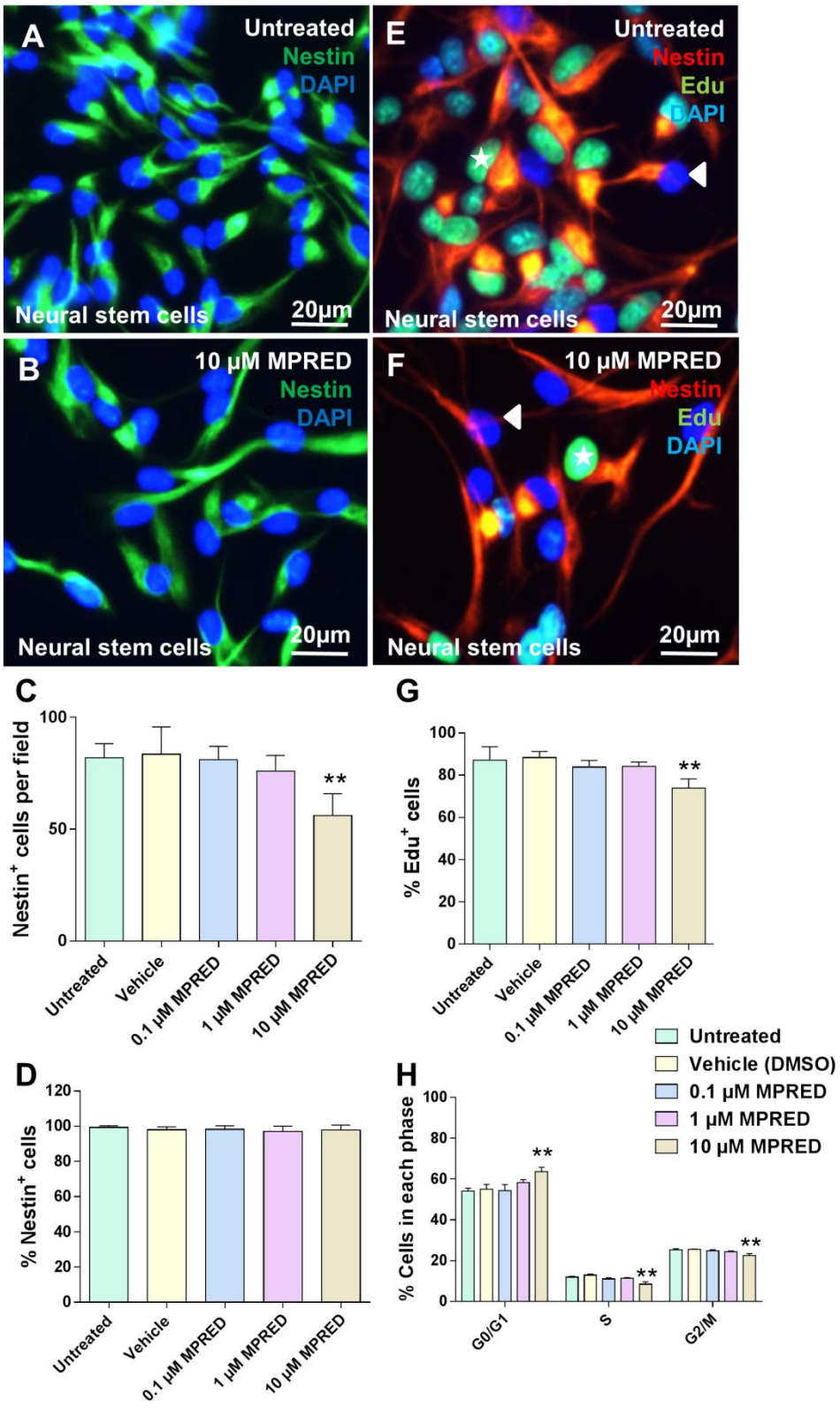

Fig. 2. Effect of MPRED on the number, proportion and proliferation of NSCs.

Fluorescence images showing nestin positive NSCs in untreated (A) and 10 μM

*MPRED treated NSCs (B). (C) Bar chart displaying the total number of NSCs per field across treatment conditions. (D) Bar chart showing the proportions of nestin positive NSC across treatment conditions. Triple merged fluorescence images depicting Edu positive NSCs in untreated (E) and 10 μM MPRED treated NSCs (F), an asterisk denotes double-labelled cells; arrowhead indicates NSCs that did not express Edu marker. (G) Bar chart showing proportions of Edu incorporating cells across treatment conditions. (H) Bar chart representing the percentage of the cells in the G0/G1, S and G2/M phase of the cell cycle. (48 h MPRED; 0.1 μM, 1 μM and 10 μM); **p<0.01 versus untreated NSCs; one-way ANOVA, Bonferroni's post-test; n = 6 for number and proportion of NSCs and n=3 for Edu assay and cell cycle analysis.*

3.3. Effects of MPRED on NSC viability and apoptosis

LIVE/DEAD staining revealed high cellular viability after MPRED treatment at all doses, comparable to control culture viability (Fig. 3A, B and C). Apoptosis of NSCs remained low (*ca.* 4%) across all conditions (Fig. 3D).

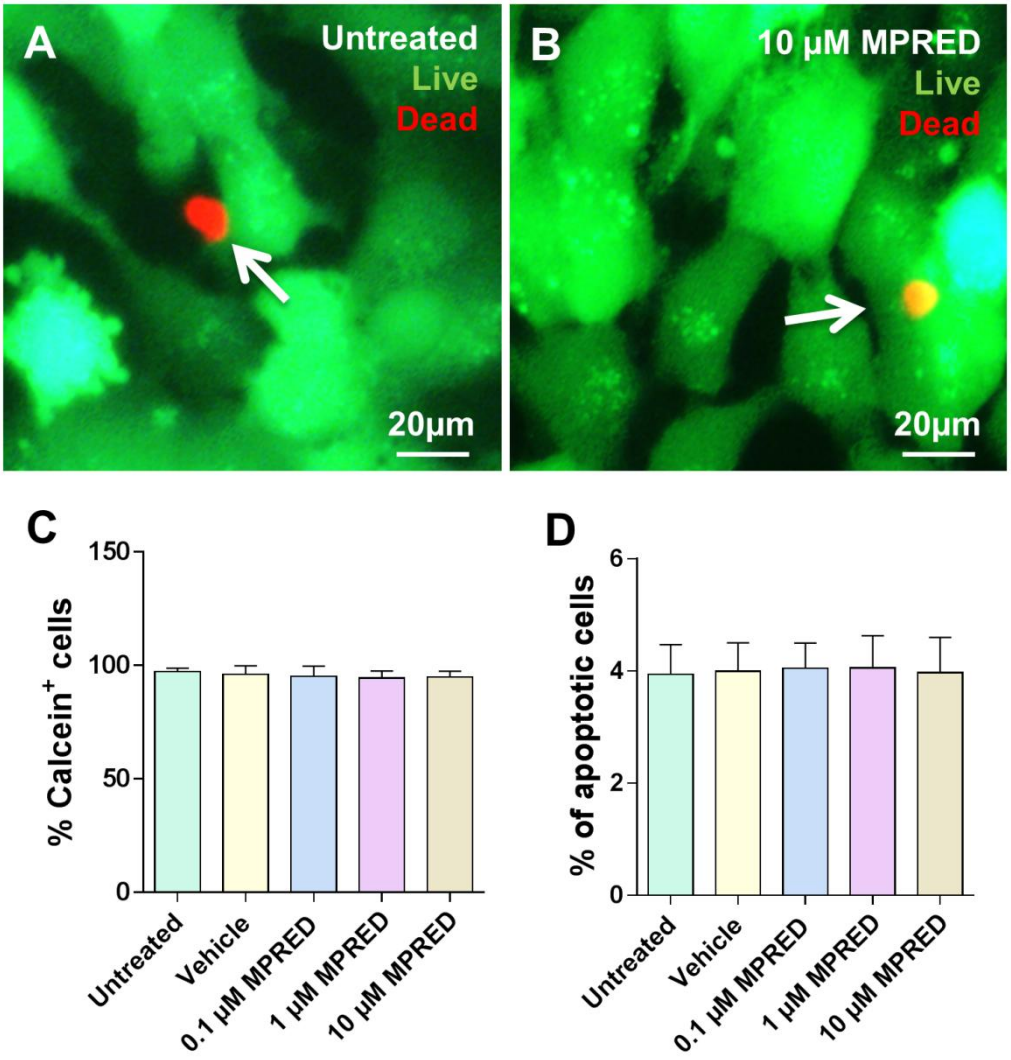

Fig. 3. Effect of MPRED on the viability and apoptosis of NSCs. *Representative LIVE/DEAD fluorescence images of untreated (A) and 10 µM MPRED treated (B) NSCs 48 h after treatment. LIVE cells appear green and DEAD cells appear red (arrows). (C) Bar chart showing the proportion of viable cells. (D) Bar chart displaying the percentage of apoptotic cells. (48 h MPRED; 0.1 µM, 1 µM and 10 µM); no significance; one-way ANOVA, Bonferroni's post-test; n = 3.*

3.4. Effect of MPRED treatment on newly generated daughter cells of NSCs

Fluorescence micrographs of astrocytes showed similar staining profiles/morphologies in all cultures, suggesting no significant MPRED-based effects (Fig. 4A and B). There was no significant difference in numbers of daughter astrocytes per field across all treatment groups (Fig. 4C). In contrast to astrocytes, 10 μM MPRED-treated NSCs produced significantly fewer neurons per field versus controls (Fig. 4D-G). 10 μM MPRED treatments also resulted in a significant reduction in axonal length versus untreated cells [28.9 ± 2.1 μm *versus* 49.9 ± 4.2 μm respectively (Fig. 4H)]. However, there was no difference in the number of oligodendrocytes generated per field after MPRED treatment. Microscopic observations suggested that oligodendrocytes in 10 μM MPRED-treated cultures had a greater membrane surface area (Fig. 4I-K). This was confirmed by the total cell area measurements wherein control cells and vehicle showed less maturation of oligodendrocytes (average area measurement 1418 ± 84.1 μm2), while 10 μM MPRED-treated cells accelerated the maturation profile of oligodendrocytes (average area measurement 1909 ± 68.4 μm2) (Fig. 4L).

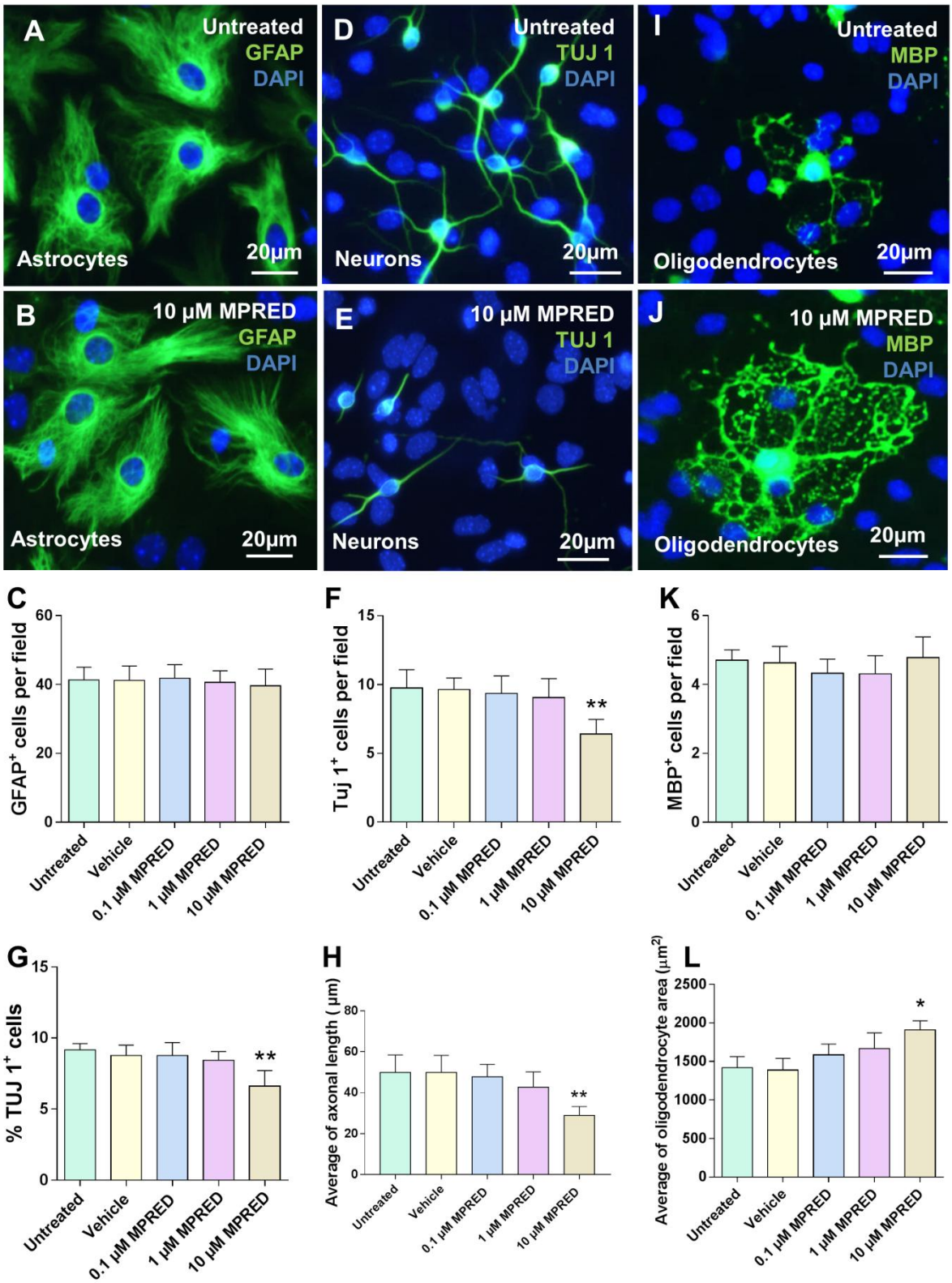

Fig. 4. Effects of MPRED treatment on newly generated daughter cells of NSCs. *Representative fluorescence micrographs depicting astrocytes generated from untreated (A) and 10 μM MPRED treated (B) differentiated NSCs. (C) Bar chart displaying the total number of GFAP$^+$ cells per field. Fluorescence micrographs of neurons derived from untreated (D) and 10 μM MPRED treated (E) differentiated NSCs. (F) Bar chart quantifying the number of TUJ 1$^+$ neurons per field across treatment conditions. (G) Bar chart showing the proportion of neurons across treatment conditions. (H) Bar chart showing the axonal length of neurons across conditions. Note reduced neuronal numbers and axonal lengths in 10 μM MPRED treated NSCs compared with untreated. Fluorescence micrographs of oligodendrocytes generated from untreated (I) and 10 μM MPRED treated (J) differentiated NSCs. Note the different morphologies and membrane surface areas of MBP$^+$ oligodendrocytes in treated cultures. (K) Bar chart showing the number of oligodendrocytes per field across treatment conditions. (L) Bar chart showing the measurement of oligodendrocyte area across treatment conditions. (9 days MPRED; 0.1 μM, 1 μM and 10 μM); **$p < 0.01$ and *$p < 0.05$ versus untreated; one-way ANOVA, Bonferroni's post-test; n = 6.*

3.5. Molecular analysis of the effects of MPRED on NSCs

Proteomic analysis was used in this study to provide an unbiased readout of molecular phenotype following MPRED treatment. A total of 3,220 quantifiable proteins from >20,000 peptide features were identified across the biological and technical replicate analyses. Pathway analysis was used to examine clustering of differentially-expressed proteins as nodes within molecular networks (Kalayou et al., 2016). A number of proteins showed significantly altered expression levels, however these were isolated entities within otherwise unaffected pathways; no entire pathways showed strong evidence of being significantly dysregulated. Whilst not linked in a canonical pathway, we next sought to identify dysregulated proteins that are known to have direct interaction with corticosteroids. There are 72 corticosteroid interacting molecules identified by IPA, 14 of which were proteins identified by the proteomics approach used here. Three of these demonstrated significant differential expression: down-regulation of matrix metalloproteinase 16 (MMP-16) and growth-associated protein 43 (GAP-43), and up regulation of cytochrome p450 51 A1 (CYP 51 A1) (Fig. 5A). Mass spectrometric relative quantification of the peptide features by Progenesis QI showed consistent patterns of regulation for the aforementioned corticosteroid primary interactors (Fig. 5B). Our results from proteomic analysis were confirmed using immunostaining to detect GAP 43. Both NSC parent cells and their differentiated cells expressed GAP 43 in treated and untreated cells. However, a significant reduction in GAP 43 expression was evident in MPRED treated NSCs and in the neurons derived from treated NSCs compared to controls. Quantification of the fluorescence intensity of GAP 43 immunostaining revealed that MPRED treated NSCs and neurons consistently demonstrated significantly lower optical density values than controls (Fig. 6).

A) corticosteroid.primary.intereactors

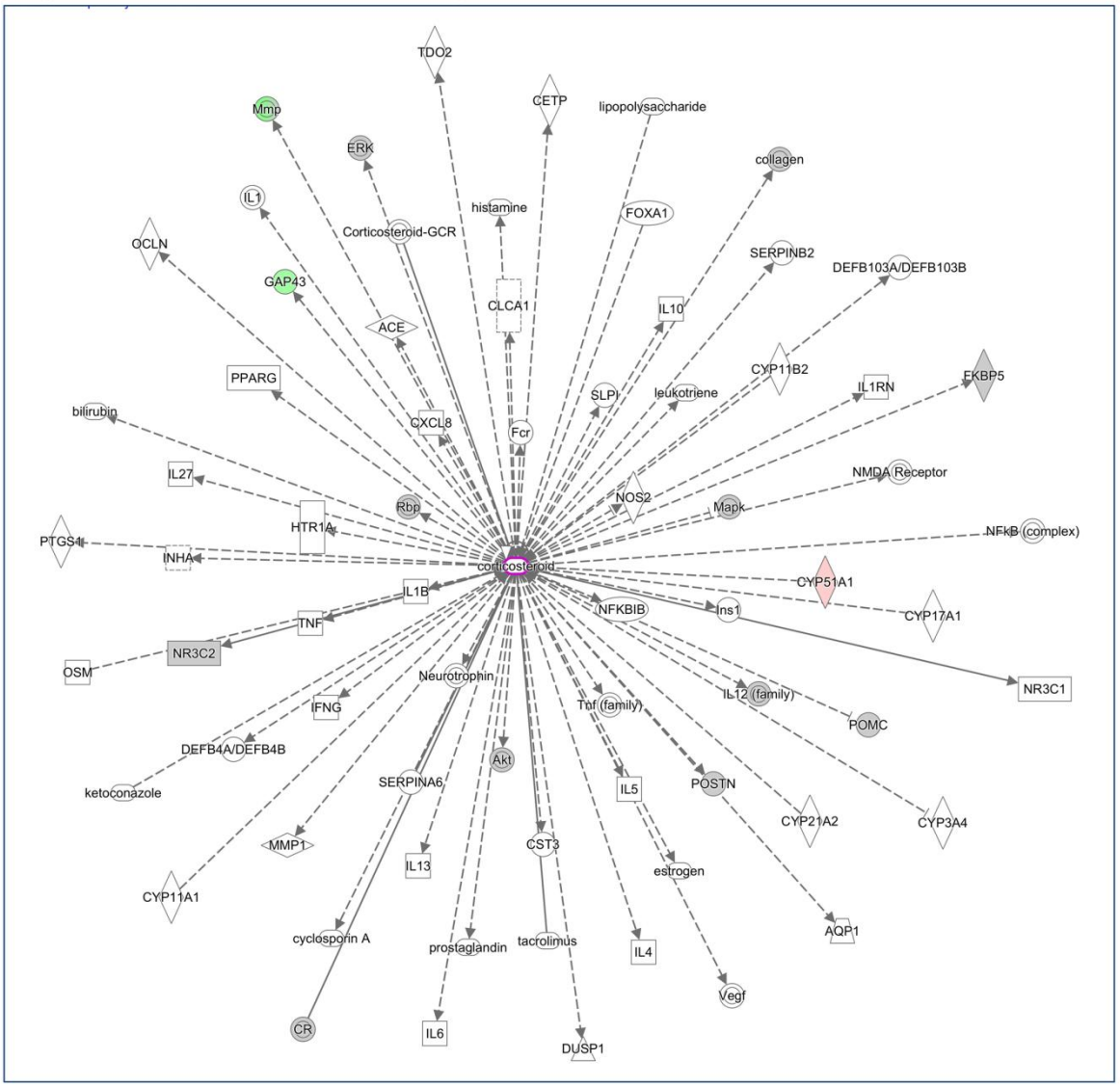

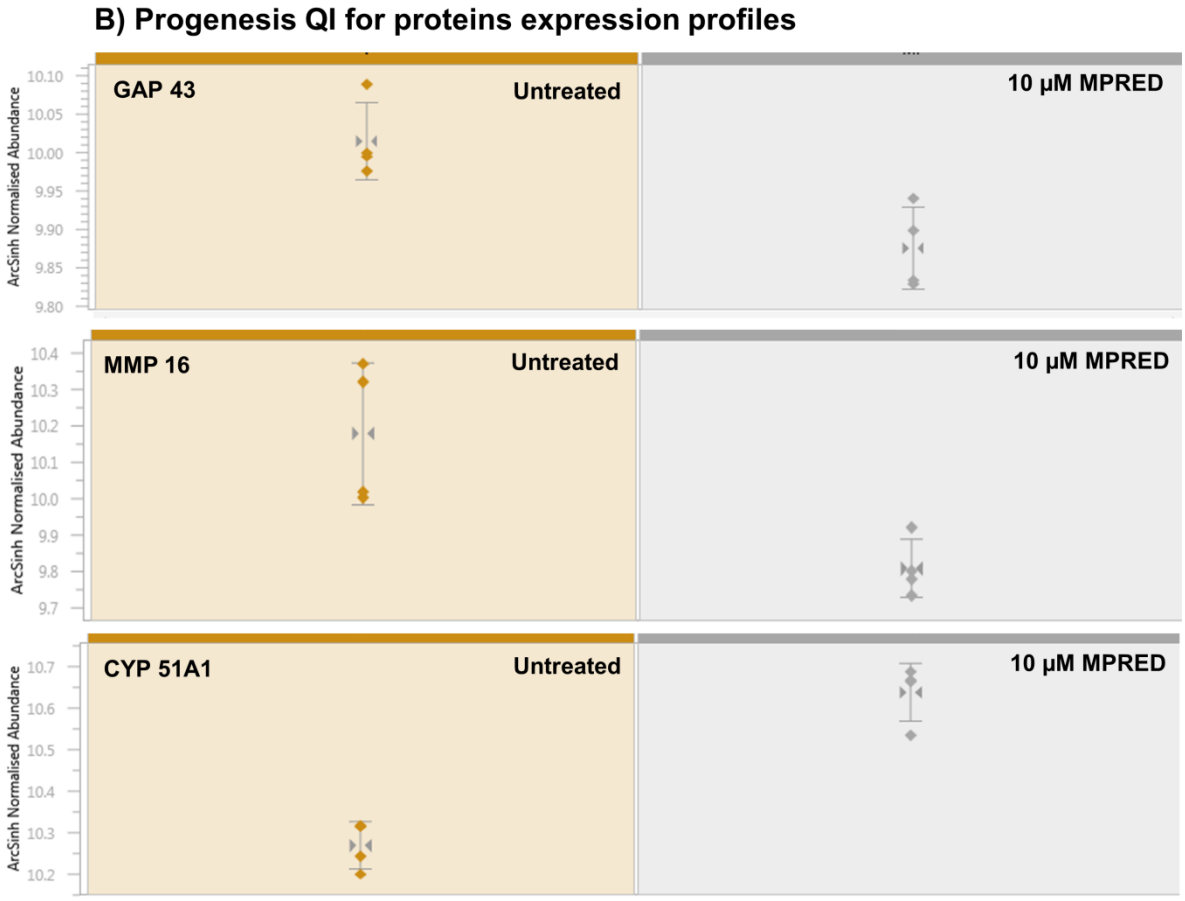

Fig. 5. Differential protein expression by NSCs following MPRED treatment. *(A) Ingenuity™ Pathway Analysis was used to cluster identified proteins according to biochemical pathways differentiating controls from MPRED-treated cells. Nodes in red indicate up-regulated proteins while those in green represent down-regulated proteins (ANOVA p<0.05, min. 2 fold). Grey nodes indicated protein detection without differential expression above the statistical threshold. (B) Progenesis QI for proteomics normalised expression profiles of GAP 43, MMP-16 and CYP51A1 illustrating protein abundance in MPRED-treated cells compared with controls, n=3.*

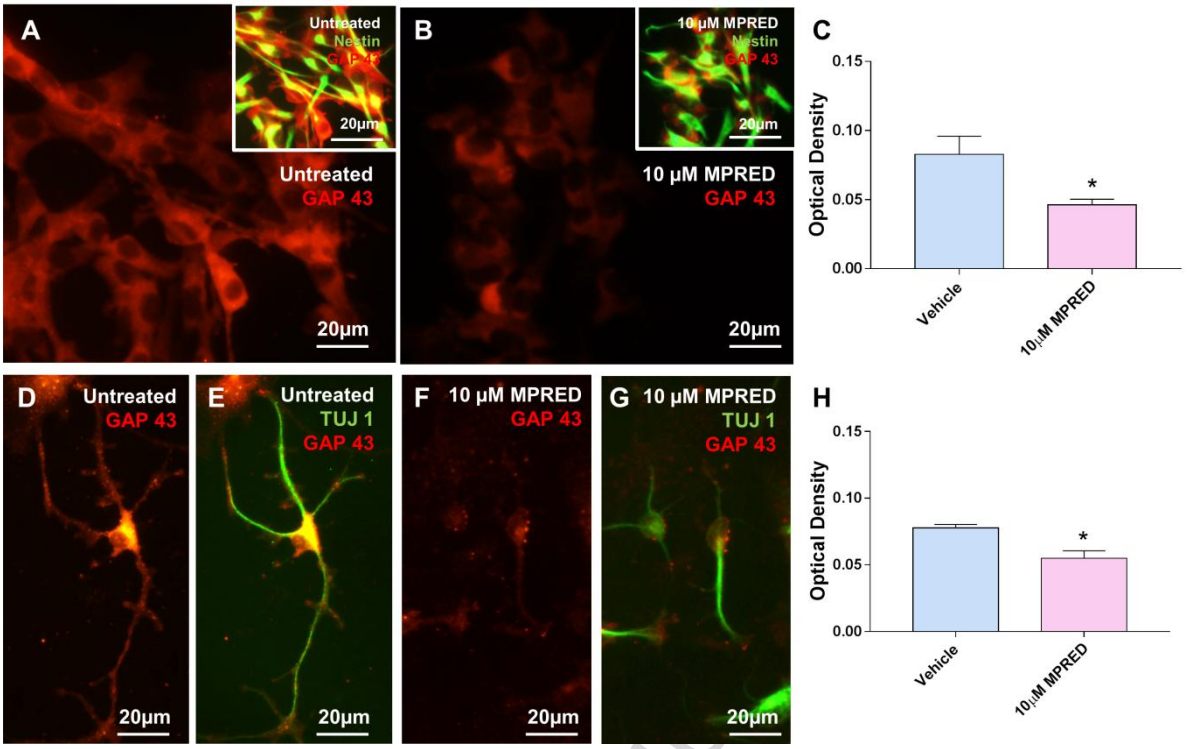

Fig. 6. NSCs and their differentiated cells show a reduction in GAP 43 expression following MPRED treatment. *Fluorescence micrographs showing GAP 43 expression in vehicle control (A) and 10 μM MPRED treated NSCs (B). Note the marked reduction in GAP 43 expression following MPRED addition. (A and B insets are the same fields with addition of nestin). (C) Bar graph showing the optical density measurements of GAP 43 expression in MPRED treated NSCs over vehicle controls. (D) Representative fluorescence micrograph of a neuron derived from untreated NSCs showing extensive GAP 43 expression. (E) Fluorescent counterpart to D showing co-localisation of GAP 43 staining with TUJ 1. (F) Representative fluorescence micrograph of neurons derived from 10 μM MPRED treated NSCs showing marked reduction in GAP 43 expression. (G) Fluorescent counterpart to F with the addition of TUJ 1. (H) Bar graph showing the optical density measurements of GAP 43 expression in MPRED of neurons derived from treated NSCs culture over vehicle controls. (48 h; 10 μM; unpaired t test; *p < 0.05, n = 3).*

4. Discussion

We have carried out dual histological and proteomic analyses to provide an insight into the molecular changes induced by CS in NSCs. The use of our dual approach to sample cellular proteins in parallel with histological observation of cells in culture provides an unbiased survey, unhindered by prior expectation. The observed concentration of a tryptic peptide, used as an analytical proxy for the net product of protein synthesis and turnover, is poorly predicted by either genome analysis or transcript levels (Lawless et al., 2016; Nagaraj et al., 2011). We consider that the work provides novel evidence to generate a key starting point to understanding the molecular mechanisms by which CSs influence an important neural cell population and its differentiated progeny. All cell types were found to express the GR receptor and therefore can be considered to be CS-responsive.

We have used SVZ derived NSCs for these experiments and the use of such cells propagated as monolayers is a widely used model in neuroscience research. The microanatomy of this region, and roles of SVZ cells in development and pathology continue to be elucidated. However, it is well established that this highly specialist niche allows for NSCs to survive, and that progenitor/stem cells from this region give rise to cells with both neuronal and glial fates. These cells have been shown to play repair roles in a range of neonatal animal models including hypoxia-ischemia, stroke, congenital cardiac disease and traumatic brain injury (Niimi and Levison, 2017). The region is also a major transplant cell source (Zuo et al., 2017) including from adult brain biopsies (Aligholi et al., 2016). Accordingly, we consider this to be an appropriate model system for the current analyses. In the future, it would be highly informative to conduct similar analyses using NSCs derived from a range of sources and brain regions.

Our study demonstrates that the highest MPRED concentration used induced a reduction in NSC number and proliferation. We observed that the percentage of Edu^+ NSCs was significantly reduced at this concentration. In parallel, cell cycle assay results suggest that CS treatment arrests the cell cycle of the NSCs at the G0/G1 phase. Our findings are broadly in line with previous studies, for example, it was demonstrated that MPRED reduced the proliferation of endogenous neural precursors (Obermair et al., 2008). Another study shows that MPRED had inhibitory effects on precursor proliferation by decreasing the levels of endothelin receptor type B protein, involved in regulating the proliferation and apoptosis of endogenous neural precursors (Li et al., 2012). Sippel and colleagues also reported that CS treatment of NPCs resulted in reduced cell proliferation and expression of a protein called BRUCE/Apollon, an apoptosis inhibitor protein family member (Sippel et al., 2009).

These studies were performed using analysis of gene expression and microarray analyses, *but as far as we are aware, no in-depth study of the influence of CS treatment upon protein expression has yet been performed in NSCs.* This is important as the correlation between transcript and protein expression changes is relatively poor, for example only 40% of altered protein expression can be directly predicted by changes in transcript levels (Vogel and Marcotte, 2013). We therefore consider our proteomic analyses beneficial in this regard, as it enables unbiased detection of molecular mechanisms potentially mediating our observed MPRED effects on NSC proliferation and differentiation. Follow up hypothesis-driven investigations can then be performed on specific identified dysregulated proteins and their phenotypic influence; these will be the goal of future research.

In line with the current findings, CSs have been found to induce a reduction in neurogenesis, axonal length and oligogenesis (Bose et al., 2010; Chetty et al., 2014; Kim et al., 2004). Recent experimental studies indicate that CS induced changes in neurogenesis are implicated in the regulation of cognition, mood, depression and emotional dysfunction (Saxe et al., 2006; Snyder et al., 2012). Our data suggest that a potential mechanism underpinning these effects could be via an early cellular re-programming of the treated parent NSCs, which in turn results in reduced GAP 43 levels – a nervous tissue–specific protein highly expressed in neurons and glial cells. The failure of expression of GAP-43 in NSCs can reduce neurogenesis, increase apoptosis of neurons and affect their maturation (Shen et al., 2004). We consider this is an important finding impacting neural development, and hence chose GAP-43 expression for further detailed immunohistochemical analysis. This corroborated proteomic data with GAP-43 in both NSCs and newly generated neurons reduced. The synthesis of GAP-43 is correlated with the development and regeneration of neurons (Hoffman, 1989), therefore GAP-43 down regulation could explain the reduced neuronal number and axonal growth in our histological analyses.

Additionally, MPRED reduced levels of MMP-16, a member of a family of proteinases which regulate biological functions such as neurogenesis, axonal extension, differentiation and cell migration in the developing and adult nervous systems. MMPs play an essential role by extracellular matrix (ECM) remodeling (Stamenkovic, 2003); the ECM and its remodeling regulate many aspects of cellular behavior such as proliferation, migration and differentiation of neural cells and NSCs (Faissner et al., 2010; Fujioka et al., 2012). The involvement of MMPs in ECM remodeling enabling axonal extension and repair after brain injury suggests a

contribution to the effects on neurogenesis and growth observed in our study; specifically, overexpression of MMPs has been shown previously to increase neurite extension and migration of neurons during neuronal development (Larsen et al., 2003; Reeves et al., 2003; Reichardt, 1991). It is not currently clear if the reduction in axonal outgrowth represents a maturation delay or a permanent alteration in neuronal morphology. In either scenario, the consequences can be predicted to be significant. This could pertain to both the establishment and maturation of appropriate neuronal circuitry during brain development, but also to processes involving complex and timed interactions with other cell types, such as oligodendrocytes during the myelination process.

MPRED treatment did not affect the proportion of NSCs differentiating into astrocytes or oligodendrocytes. In contrast, Sabolek *et al.* observed that CS exposure leads to a reduction in astrocyte differentiation (Sabolek et al., 2006). We suggest that the observed differences may be attributable to the differences in both methodology and origin of NSCs between the two studies. However, MPRED was found to accelerate the maturation of newly generated oligodendrocytes, a finding with potential implications for the myelination process. Jenkins *et al.* studied direct actions of CS on oligodendrocytes and their progenitors, the oligodendrocyte precursor cells (OPCs) in culture. No effects were found on OPC proliferation and survival, or oligodendrocyte maturation (Jenkins et al., 2014). However, we suggest that the known CS effects on myelin genesis (Chari et al., 2006; Clarner et al., 2011) may alternatively be mediated via changes in the interactions of newly generated oligodendrocytes with axons in the developing nervous system; this is normally a highly spatially and temporally controlled process. Premature maturation of oligodendrocytes can be predicted to result in aberrant myelination. Our findings

suggest a possible link between the upregulation of key protein involved in cholesterol biosynthesis, CYP51A1 (aka lanosterol 14 α-demethylase) and the maturation of oligodendrocytes. CYP51A1 is involved in important steps in the biosynthesis of cholesterol (Björkhem et al., 2004; Debeljak et al., 2003) which is which is found in high levels in myelin, (Orth and Bellosta, 2012). We therefore suggest that alterations in cholesterol biosynthesis could be associated with impairments to oligodendrocyte development and the myelination process.

In ongoing work, our laboratory has tested two more clinically relevant and widely used CSs - dexamethasone and prednisone in identical studies. Overall, a similar profile was observed across all three preparations, suggesting the need for careful evaluation of the effects of this major class of drugs on development and fate of NSCs.

5. Conclusion

In summary, our analyses suggest that the down regulation of major neural development proteins MMP-16 and GAP-43, along with MPRED induced upregulation of CYP51A1 proteins involved in cholesterol synthesis, provides an explanation for the observed histological effects of MPRED on NSCs. The clustering of these proteins within a single network suggests MPRED treatment acts by altering a common upstream regulator of these proteins, rather than individual disparate nodes being affected in unrelated molecular pathways. Detailed analysis of the relative contributions of the multiple competing cellular processes (transcriptional, co-transcriptional, translational, post-translational or protein degradation) which result in net protein concentration is beyond the scope of the current study, but this finding suggests opportunities for further investigation of MPRED influence on NSCs. Our findings highlight the need for development of new immunosuppressive agents and treatment regimens to reduce adverse neurological effects of CSs on stem cell populations of the nervous system.

Acknowledgements

This study was supported by was supported by the Iraqi Ministry of Higher Education and Scientific Research (MOHESR). LS was supported by the British Mass Spectrometry Society Summer Studentships scheme and by an EPSRC-funded Centre for Innovative Manufacturing in Regenerative Medicine Summer Studentship Award. CA was funded by an EPSRC-ETERM Fellowship.

References

Adams, C.F., Pickard, M.R., Chari, D.M., 2013. Magnetic nanoparticle mediated transfection of neural stem cell suspension cultures is enhanced by applied oscillating magnetic fields. Nanomedicine Nanotechnology, Biol. Med. 9, 737–741. doi:10.1016/j.nano.2013.05.014

Aligholi, H., Hassanzadeh, G., Gorji, A. and Azari, H., 2016. A Novel Biopsy Method for Isolating Neural Stem Cells from the Subventricular Zone of the Adult Rat Brain for Autologous Transplantation in CNS Injuries. Injury Models of the Central Nervous System: Methods and Protocols, pp.711-731

Ansari, D., Andersson, R., Bauden, M., Andersson, B., Connolly, J., Welinder, C., Sasor, A., Marko-Varga, G., 2015. Protein deep sequencing applied to biobank samples from patients with pancreatic cancer.

Ayroldi, E., Cannarile, L., Migliorati, G., Nocentini, G., Delfino, D. V, Riccardi, C., 2012. Mechanisms of the anti-inflammatory effects of glucocorticoids: genomic and nongenomic interference with MAPK signaling pathways. FASEB J. 26, 4805–20. doi:10.1096/fj.12-216382

Björkhem, I., Meaney, S., Fogelman, A.M., 2004. Brain Cholesterol: Long Secret Life behind a Barrier. Arterioscler. Thromb. Vasc. Biol. 24, 806–815. doi:10.1161/01.ATV.0000120374.59826.1b

Bose, R., Moors, M., Tofighi, R., Cascante, a, Hermanson, O., Ceccatelli, S., 2010. Glucocorticoids induce long-lasting effects in neural stem cells resulting in senescence-related alterations. Cell Death Dis. 1, e92. doi:10.1038/cddis.2010.60

Burniston, J., Connolly, J., Kainulainen, H., Britton, S., Koch, L., 2014. Label-free profiling of skeletal muscle using high-definition mass spectrometry. Proteomics. 14, 2339–2344. doi:10.1038/nmeth.2250.Digestion

Chari, D., 2014. How do corticosteroids influence myelin genesis in the central nervous system? Neural Regen. Res. 9, 909–911. doi:10.4103/1673-5374.133131

Chari, D.M., Zhao, C., Kotter, M.R., Blakemore, william F., Frankiln, R.J.M., 2006. Corticosteroids delay remyelination of experimental demyelination in the rodent central nervous system. J. Neurosci. Res. 83, 594–605. doi:10.1002/jnr

Chetty, S., Friedman, A., Taravosh-Lahn, K., Kirby, E.D., Mirescu, C., Guo, F., Krupik, D., Tsai, M.-K., 2014. Stress and glucocorticoids promote oligodendrogenesis in the adult hippocampus. Mol Psychiatry 19, 1275–1283. doi:10.1017/S0954579414000868.Child-evoked

Clarner, T., Parabucki, A., Beyer, C., Kipp, M., 2011. Corticosteroids Impair Remyelination in the Corpus Callosum of Cuprizone-Treated Mice. J. Neuroendocrinol. 23, 601–611. doi:10.1111/j.1365-2826.2011.02140.x

Debeljak, N., Fink, M., Rozman, D., 2003. Many facets of mammalian lanosterol 14α-demethylase from the evolutionarily conserved cytochrome P450 family CYP51. Arch. Biochem. Biophys. 409, 159–171. doi:10.1016/S0003-9861(02)00418-6

Faissner, A., Pyka, M., Geissler, M., Sobik, T., Frischknecht, R., Gundelfinger, E.D., Seidenbecher, C., 2010. Contributions of astrocytes to synapse formation and maturation - Potential functions of the perisynaptic extracellular matrix. Brain Res. Rev. 63, 26–38. doi:10.1016/j.brainresrev.2010.01.001

Fujioka, H., Dairyo, Y., Yasunaga, K.I., Emoto, K., 2012. Neural functions of matrix metalloproteinases: Plasticity, neurogenesis, and disease. Biochem. Res. Int. doi:10.1155/2012/789083

Han, Z., Lat, I., Pollard, S.R., 2014. Safety and Efficacy of Corticosteroid Use in Neurologic Trauma. J Pharm Pr. 27, 487–95. doi:10.1177/0897190013516500

Heberden, C., Meffray, E., Goustard-Langelier, B., Maximin, E., Lavialle, M., 2013. Dexamethasone inhibits the maturation of newly formed neurons and glia supplemented with polyunsaturated fatty acids. J. Steroid Biochem. Mol. Biol. 138, 395–402. doi:10.1016/j.jsbmb.2013.07.010

Heine, V.M., Rowitch, D.H., 2009. Hedgehog signaling has a protective effect in glucocorticoid-induced mouse neonatal brain injury through an 11 β HSD2-dependent mechanism. J. Clin. Invest 119, 267–277. doi:10.1172/JCI36376.cell

Hoffman, P.N., 1989. Expression of GAP-43 , a Rapidly Transported Growth-Associated Neurons GAP TUB. J. Neurosci. 9, 893–897.

Jenkins, S.I., Pickard, M.R., Khong, M., Smith, H.L., Mann, C.L. a, Emes, R.D., Chari, D.M., 2014. Identifying the cellular targets of drug action in the central nervous system following corticosteroid therapy. ACS Chem. Neurosci. 5, 51–63. doi:10.1021/cn400167n

Kalayou, S., Granuma, C., Berntsena, H.F., Grosetha, P.K., Verhaegena, S., Connollyc, L., Brandtd, I., Antonio de Souzae, G., Ropstad, E., 2016. Label-free based quantitative proteomics analysis of primary neonatal porcine Leydig cells exposed to the persistent contaminant 3-methylsulfonyl-DDE.

Kim, J. Bin, Ju, J.Y., Kim, J.H., Kim, T.-Y., Yang, B.-H., Lee, Y.-S., Son, H., 2004.

Dexamethasone inhibits proliferation of adult hippocampal neurogenesis in vivo and in vitro. Brain Res. 1027, 1–10. doi:10.1016/j.brainres.2004.07.093

Larsen, P.H., Wells, J.E., Stallcup, W.B., Opdenakker, G., Yong, V.W., 2003. Matrix metalloproteinase-9 facilitates remyelination in part by processing the inhibitory NG2 proteoglycan. J. Neurosci. 23, 11127–11135. doi:23/35/11127 [pii]

Lawless, C., Holman, S.W., Brownridge, P., Lanthaler, K., Victoria, M., Watkins, R., Hammond, D.E., Miller, R.L., Sims, P.F.G., Grant, C.M., Eyers, C.E., Beynon, R.J., Hubbard, S.J., 2016. Direct and Absolute Quantification of over 1 80 0 Yeast Proteins via Selected Reaction Monitoring. Mol. Cell. Proteomics 15, 1309–1322. doi:10.1074/mcp.M115.054288

Li, S.-Y., Wang, P., Tang, Y., Huang, L., Wu, Y.-F., Shen, H.-Y., 2012. Analysis of methylprednisolone-induced inhibition on the proliferation of neural progenitor cells in vitro by gene expression profiling. Neurosci. Lett. 526, 154–9. doi:10.1016/j.neulet.2012.07.047

Mazzini, L., Gelati, M., Profico, D.C., Sgaravizzi, G., Projetti Pensi, M., Muzi, G., Ricciolini, C., Rota Nodari, L., Carletti, S., Giorgi, C., Spera, C., Domenico, F., Bersano, E., Petruzzelli, F., Cisari, C., Maglione, A., Sarnelli, M.F., Stecco, A., Querin, G., Masiero, S., Cantello, R., Ferrari, D., Zalfa, C., Binda, E., Visioli, A., Trombetta, D., Novelli, A., Torres, B., Bernardini, L., Carriero, A., Prandi, P., Servo, S., Cerino, A., Cima, V., Gaiani, A., Nasuelli, N., Massara, M., Glass, J., Sorarù, G., Boulis, N.M., Vescovi, A.L., 2015. Human neural stem cell transplantation in ALS: initial results from a phase I trial. J. Transl. Med. 13, 371. doi:10.1186/s12967-014-0371-2

Moors, M., Bose, R., Johansson-Haque, K., Edoff, K., Okret, S., Ceccatelli, S., 2012. Dickkopf 1 mediates glucocorticoid-induced changes in human neural progenitor cell proliferation and differentiation. Toxicol. Sci. 125, 488–95. doi:10.1093/toxsci/kfr304

Nagaraj, N., Wisniewski, J.R., Geiger, T., Cox, J., Kircher, M., Kelso, J., Paabo, S., Mann, M., 2011. Deep proteome and transcriptome mapping of a human cancer cell line. Mol. Syst. Biol. 7, 548. doi:10.1038/msb.2011.81

Niimi, Y. and Levison, S.W., 2017. Pediatric brain repair from endogenous neural stem cells of the subventricular zone. Pediatric research. doi: 10.1038/pr.2017.261

Obermair, F.-J., Schröter, A., Thallmair, M., 2008. Endogenous neural progenitor cells as therapeutic target after spinal cord injury. Physiology 23, 296–304. doi:10.1152/physiol.00017.2008

Orth, M., Bellosta, S., 2012. Cholesterol: Its regulation and role in central nervous system disorders. Cholesterol 2012. doi:10.1155/2012/292598

Reeves, T.M., Prins, M.L., Zhu, J., Povlishock, J.T., Phillips, L.L., 2003. Matrix metalloproteinase inhibition alters functional and structural correlates of deafferentation-induced sprouting in the dentate gyrus. J. Neurosci. 23, 10182–9. doi:23/32/10182 [pii]

Reichardt, L., 1991. Extracellular Matrix Molecules And Their Receptors: Functions In Neural Development. Annu. Rev. Neurosci. 14, 531–570. doi:10.1146/annurev.neuro.14.1.531

Rhen, T., Cidlowski, J. a, 2005. Antiinflammatory action of glucocorticoids-new

mechanisms for old drugs. N. Engl. J. Med. 353, 1711–23. doi:10.1056/NEJMra050541

Riedemann, T., Patchev, A. V, Cho, K., Almeida, O.F.X., 2010. Corticosteroids: way upstream. Mol. Brain 3, 2. doi:10.1186/1756-6606-3-2

Rodriguez-Suarez, E., Hughes, C., Gethings, L., Giles, K., Wildgoose, J., Stapels, M., Fadgen, K.E., Geromanos, S.J., Vissers, J.P.C., Elortza, F., Langridge, J.I., 2013. An Ion Mobility Assisted Data Independent LC-MS Strategy for the Analysis of Complex Biological Samples. Curr. Anal. Chem. 9, 199–211. doi:10.2174/157341113805218947

Sabolek, M., Anna, H., Johannes, S., Alexander, S., 2006. Dexamethasone blocks astroglial differentiation from neural precursor cells.

Saxe, M.D., Battaglia, F., Wang, J.-W., Malleret, G., David, D.J., Monckton, J.E., Garcia, A.D.R., Sofroniew, M. V, Kandel, E.R., Santarelli, L., Hen, R., Drew, M.R., 2006. Ablation of hippocampal neurogenesis impairs contextual fear conditioning and synaptic plasticity in the dentate gyrus. Proc. Natl. Acad. Sci. U. S. A. 103, 17501–6. doi:10.1073/pnas.0607207103

Shen, Y., Mani, S., Meiri, K.F., 2004. Failure to express GAP-43 leads to disruption of a multipotent precursor and inhibits astrocyte differentiation. Mol. Cell. Neurosci. 26, 390–405. doi:10.1016/j.mcn.2004.03.004

Shinwell, E.S., Eventov-Friedman, S., 2009. Impact of perinatal corticosteroids on neuromotor development and outcome: Review of the literature and new meta-analysis. Semin. Fetal Neonatal Med. 14, 164–170. doi:10.1016/j.siny.2008.12.001

Silva, J.C., Gorenstein, M. V, Li, G.-Z., Vissers, J.P.C., Geromanos, S.J., 2005. Absolute Quantification of Proteins by LCMSE: A Virtue of Parallel ms Acquisition. Mol. Cell. Proteomics 5, 144–156. doi:10.1074/mcp.M500230-MCP200

Sippel, M., Rajala, R., Korhonen, L., Bornhauser, B., Sokka, A.-L., Naito, M., Lindholm, D., 2009. Dexamethasone regulates expression of BRUCE/Apollon and the proliferation of neural progenitor cells. FEBS Lett. 583, 2213–7. doi:10.1016/j.febslet.2009.06.018

Skardelly, M., Glien, A., Groba, C., Schlichting, N., Kamprad, M., Meixensberger, J., Milosevic, J., 2013. The influence of immunosuppressive drugs on neural stem/progenitor cell fate in vitro. Exp. Cell Res. 319, 3170–3181. doi:10.1016/j.yexcr.2013.08.025

Snyder, J.S., Soumier, A., Brewer, M., Pickel, J., Cameron, H.A., 2012. Adult hippocampal neurogenesis buffers stress responses and depressive behavior. Nature 476, 458–461. doi:10.1038/nature10287.Adult

Stamenkovic, I., 2003. Extracellular matrix remodelling: the role of matrix metalloproteinases. J. Pathol. 200, 448–464. doi:10.1002/path.1400

Sun, Y., Kong, W., Falk, A., Hu, J., Zhou, L., Pollard, S., Smith, A., 2009. C0D133 (Prominin) negative human neural stem cells are clonogenic and tripotent. PLoS One 4, 16–18. doi:10.1371/journal.pone.0005498

Sundberg, M., Savola, S., Hienola, A., Korhonen, L., Lindholm, D., 2006. Glucocorticoid hormones decrease proliferation of embryonic neural stem cells through ubiquitin-mediated degradation of cyclin D1. J. Neurosci. 26, 5402–10.

doi:10.1523/JNEUROSCI.4906-05.2006

Zuo, F., Xiong, F., Wang, X., Li, X., Wang, R., Ge, W. and Bao, X., 2017. Intrastriatal Transplantation of Human Neural Stem Cells Restores the Impaired Subventricular Zone in Parkinsonian Mice. Stem Cells, 35(6), pp.1519-1531.

Vogel, C., Marcotte, E.M., 2013. Insights into regulation of protein abundance from proteomics and transcriptomis analyses. Nat. Rev. Genet. 13, 227–232. doi:10.1038/nrg3185.Insights

Highlights:

- Treatment of NSCs with a widely used clinical corticosteroid showed that proliferation of neural stem cells was reduced by the treatment.
- Genesis of neurons and axonal length were reduced, while oligodendrocyte maturation was increased after corticosteroids treatment.
- First investigation into underlying mechanisms by proteomic analysis showed corticosteroid induced downregulation of growth associated protein 43 and matrix metallopeptidase 16 with upregulation of the cytochrome P450 family 51 subfamily A member 1